fishes

MDPI

Article

Transcriptome Analysis of Gill Tissues from *Neptunea cumingii* in Different Seasons

Yifan Zhang [1,†], Dandan Zhang [2,†], Ying Tian [1], Junxia Mao [1], Yang Liu [1,*] and Zhenlin Hao [1,*]

[1] Key Laboratory of Mariculture and Stock Enhancement in North China's Sea, Dalian Ocean University, Ministry of Agriculture, Dalian 116023, China; 13190456321@163.com (Y.Z.); tianying@dlou.edu.cn (Y.T.); maojunxia@dlou.edu.cn (J.M.)
[2] College of Life Science, Tarim University, Aral 843300, China; 18449600718@163.com
* Correspondence: liuyang@dlou.edu.cn (Y.L.); haozhenlin@dlou.edu.cn (Z.H.)
† These authors have contributed equally to this work.

Abstract: *Neptunea cumingii* is an economically important marine shellfish found in the Yellow and Bohai Seas areas of China. In this study, samples of *Neptunea cumingii* were collected in Zhangzidao and Yantai during spring, summer, autumn, and winter to clarify the gene expression patterns and regulatory mechanisms in their gills in different seasons. Transcriptome analysis was conducted using *Neptunea cumingii* gill tissues, and genes with significantly different expression levels were extracted for functional verification. The most genes with differences in expression (DEGs) were found in comparisons of the winter and summer samples. Gene enrichment analysis based on Gene Ontology and Kyoto Encyclopedia of Genes and Genomes terms showed that these DEGs were mainly involved in immune and metabolic pathways, and they had significant effects on oxidative stress, body metabolism, and protein synthesis in *Neptunea cumingii*. Further screening of DEGs identified thirty-four genes related to temperature regulation, comprising thirteen genes with roles in innate immunity in shellfish, twelve genes related to oxidative stress, and nine genes related to protein synthesis and energy metabolism. Eleven DEGs were randomly selected for qPCR verification, and the results were consistent with the transcriptome analysis results. In summary, the transcriptome results differed significantly between seasons in the gill tissues of *Neptunea cumingii*. The expression levels of immune regulatory genes could be promoted in *Neptunea cumingii* during the high temperature season, whereas the expression of these genes may be inhibited in the low temperature season. The results obtained in this study provide insights into the molecular defense mechanisms that might allow *Neptunea cumingii* to adapt to climate change.

Keywords: immune function; *Neptunea cumingii*; oxidative stress; seasonal variation

Key Contribution: Through transcriptome sequencing technology, this study provides, for the first time, evidence supporting the presence of molecular adaptations to seasonal temperature changes in *Neptunea cumingii*, revealing significant expression of genes associated with different biological pathways; most of these genes are related to immune regulation and energy metabolism.

check for updates

Citation: Zhang, Y.; Zhang, D.; Tian, Y.; Mao, J.; Liu, Y.; Hao, Z. Transcriptome Analysis of Gill Tissues from *Neptunea cumingii* in Different Seasons. *Fishes* **2023**, *8*, 549. https://doi.org/10.3390/fishes8110549

Academic Editor: Alberto Pallavicini

Received: 20 October 2023
Revised: 8 November 2023
Accepted: 10 November 2023
Published: 11 November 2023

1. Introduction

Neptunea cumingii (Gastropoda, Probranchia, Neptunea, Mothidae) is a carnivorous snail and the most economically important shellfish along the northern coast of China [1]. The meat of *Neptunea cumingii* is nutritious and an ideal source of dietary protein and fat [2], and it is greatly favored by consumers. Previous studies of *Neptunea cumingii* mainly focused on its distribution [3], growth and reproduction [4,5], genetic diversity [6], and the effects of salinity and dissolved oxygen on its physiological activities [7,8], whereas few have considered the mechanism associated with temperature adaptation by *Neptunea cumingii* [9].

Temperature is an important environmental factor that affects the metabolism, growth, and life activities of marine bivalves [10]. When shellfish perceive short-term fluctuations in temperature or long-term seasonal changes, they will adapt to the change in the environmental temperature by actively adjusting their physiological and biochemical activities [11]. Previous studies have investigated the physical response mechanisms in various shellfish under changing environmental temperatures and have shown that the expression of heat shock proteins (HSPs) is stimulated in shellfish to maintain cell homeostasis under high temperature conditions, where the response to damage also involves the activation of immune cells and accelerated metabolism. Under low-temperature conditions, shellfish respond to oxidative stress by stimulating the production of glutathione S-transferases (GSTs), such as in *Ruditapes philippinarum* [10], *Patinopecten yessoensis* [12,13], and *Chlamys farreri* [13]. However, the regulatory mechanism that allows *Neptunea cumingii* to adapt to seasonal temperature changes has not been reported previously. Therefore, in this study, we conducted transcriptome sequencing using gill tissues collected from *Neptunea cumingii* in different seasons with natural temperature variability. Genes related to environmental adaptation were screened, and the functions of these genes were verified in order to understand the mechanisms that allow *Neptunea cumingii* to adapt to seasonal temperature changes and thus provide a reference to improve the production of *Neptunea cumingii.*

2. Materials and Methods

2.1. Experimental Materials

In this study, samples of *Neptunea cumingii* were collected from Zhangzidao Island in Dalian City (ZZ, longitude: 121.66° E, latitude: 39.054° N) and Bajiao Port in Yantai City (YT, longitude: 121.15° E, latitude: 37.641° N), China (Figure 1). In particular, samples were collected during 2021 in the spring (C), summer (X), autumn (Q), and winter (D) (Table 1). Sample data include the temperature situation in China, the weather http://www.weather.com.cn/ query (accessed on 28 March 2021; 25 June 2021; 23 September 2021; 7 December 2021), and record in time. Twenty individuals were collected at each site each quarter, divided into four parallel experimental groups of five, washed with sterilized sea water, immediately dissected with anatomical scissors and scalpels, and their gill tissue was taken and quickly frozen in liquid nitrogen. Subsequently, the samples were transported to the Northern Key Laboratory of Mariculture of the Ministry of Agriculture and Rural Affairs and stored in a −80 °C frozen refrigerator for further analysis. Five samples of the same size from each group were mixed.

Table 1. Summary of *Neptunea cumingii* samples used in the study.

Locations	Seasons	Number	Date	Temperature
Zhangzidao	Spring	20	28 March 2021	7 °C
	Summer	20	25 June 2021	21 °C
	Autumn	20	23 September 2021	18 °C
	Winter	20	7 December 2021	5 °C
Yantai	Spring	20	28 March 2021	8 °C
	Summer	20	25 June 2021	23 °C
	Autumn	20	23 September 2021	19 °C
	Winter	20	7 December 2021	6 °C

2.2. Experimental Methods

2.2.1. RNA Extraction, Library Preparation, and Illumina Sequencing

The total amounts and integrity of RNA were assessed using an RNA Nano 6000 Assay Kit with the Bioanalyzer 2100 system (Agilent Technologies, Santa Clara, CA, USA) according to the manufacturer's protocol. Briefly, mRNA was purified from total RNA using poly-T oligo-attached magnetic beads. First-strand cDNA was synthesized using random hexamer primers and M-MuLV reverse transcriptase, before applying RNaseH to degrade the RNA. Second-strand cDNA synthesis was then performed using DNA polymerase I

and dNTPs. The library fragments were purified with the AMPure XP system (Beckman Coulter, Brea, CA, USA). After PCR amplification, the PCR products were purified using AMPure XP beads to obtain the final library. Then, these libraries were sequenced on the illumina NovaSeq 6000 (illumina, USA) and 150 bp paired-end reads were generated. Transcriptome sequencing and analysis was performed by Novogene Biotechnology Co., Ltd. (Beijing, China).

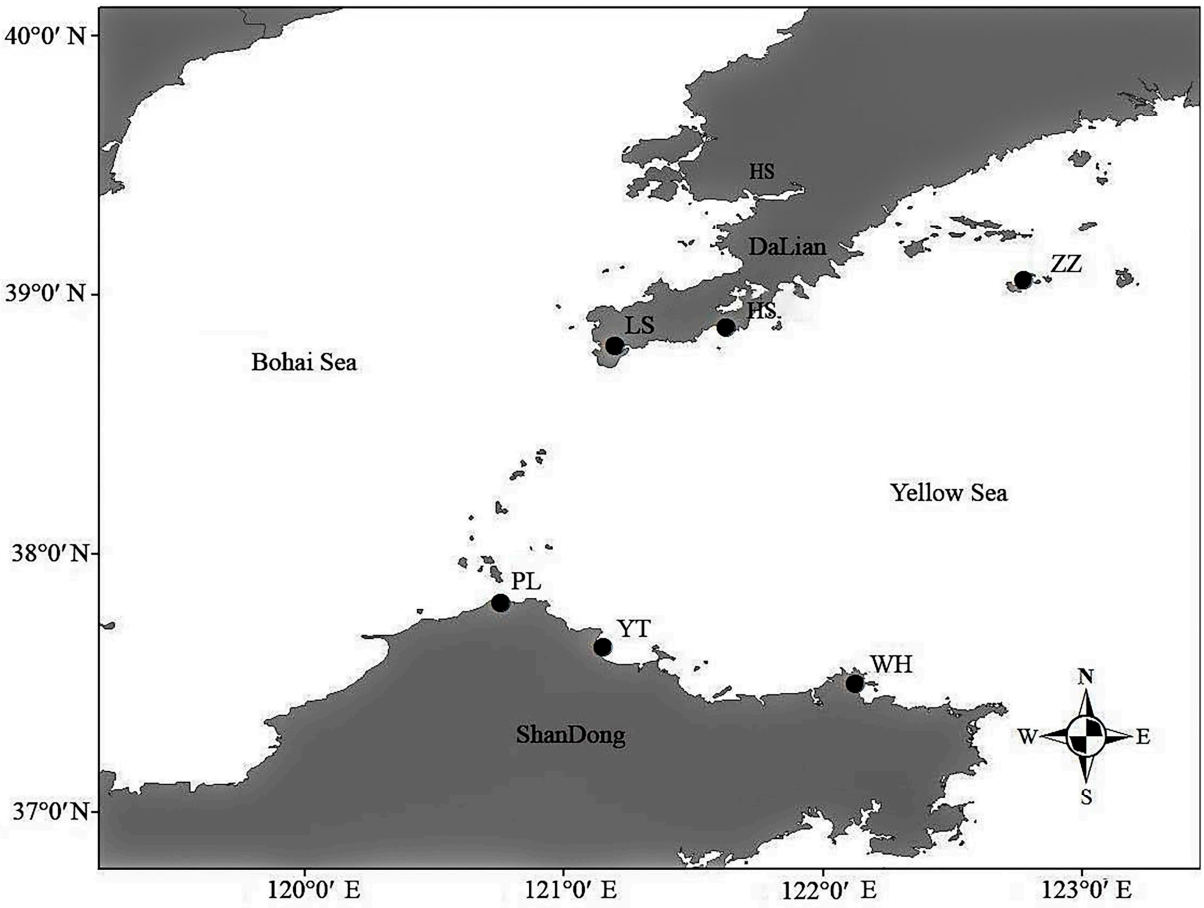

Figure 1. Collection locations of *Neptunea cumingii* [6].

2.2.2. Data Filtering and De Novo Assembly

The image data measured using the high-throughput sequencer are converted into sequence data (reads) via CASAVA base recognition. Raw data (raw reads) of fastq format were firstly processed through in-house perl scripts. By removing the reads with the adapter, reads containing N (N indicates that base information cannot be determined) and low-quality reads (reads with Qphred $\leq$ 20 base number accounting for more than 50% of the entire read length) were removed to filter the raw data and thus clean reads. After removing adaptor and low-quality sequences, the clean reads were assembled into expressed sequence tag clusters (contigs) and de novo assembled into transcript using Trinity (version: 2.6.6) in the paired-end method. Using the spliced transcriptome as a reference sequence (Ref), RSEM software [14] was used to compare the clean reads of each sample to the Ref. reads with a comparison mass value lower than 10, and those without paired comparison were filtered out, respectively. Reads were compared to multiple regions of the genome, and then the read count numbers were converted to fragments per kilobase million (FPKM). Gene function was annotated based on the following databases: NCBI non-redundant protein sequences (Nr), NCBI non-redundant nucleotide sequences (Nt), Protein family (Pfam), Clusters of Orthologous Groups of proteins (KOG/COG), a manually

annotated and reviewed protein sequence database (Swiss-Prot), KEGG Ortholog database (KO), and Gene Ontology (GO).

2.2.3. DEGs Screening and Enrichment Analysis

DEGs were identified using the Benjamini and Hochberg procedure to control FDR (false discovery rate; padj < 0.05) determining by this way significantly differential expression. Hierarchical cluster analysis of DEGs was performed to explore transcript expression patterns. Based on the hypergeometric distribution principle, GOseq (1.10.0) and KOBAS (v2.0.12) software were used for GO functional enrichment analysis and KEGG pathway enrichment analysis of DEGs.

2.2.4. Quantitative Real-Time-PCR Validation

To examine the reliability of the RNA-Seq results, we randomly selected 11 DEGs from 34 temperature-related DEGs for qRT-PCR validation, including caspase activity and apoptosis inhibitor 1 (CAAP1), toll-like receptor 8 (TLR8), toll-like receptor 13 (TLR13), toll-like receptor 3 (TLR3), heat shock protein 70 (HSP70), heat shock protein 90 (HSP90), calreticulin (CRT), phosphatidylinositol 3,4,5-trisphosphate 5-phosphatase 2 (Ptp2), glutathione S-transferase kappa 1-like (GSTK1), interferon regulatory factor 5 (IRF5), and mitogen-activated protein kinase kinase 6 (MAP2K6). The primers were designed using Primer Premier 5.0, with lengths of 18–27 bp, GC (ratio of two bases, guanine and cytosine, to the total base) content of 45–55%, and annealing temperature of 50–70 °C [15] and synthesized by Sangon Biotech Co., Ltd. (Shanghai, China). The RNA was reverse transcribed to cDNA using TIANGEN® FastKing gDNA Dispelling RT SuperMix (Tiangen Biotech, China). Suitable primers were designed using Primer 5.0 (Table 2) and synthesized by Sangon Biotech Co., Ltd. (Shanghai, China). qRT-PCR was performed with TIANGEN® Talent qPCR PreMix (SYBR Green) (Tiangen Biotech, China) on a Roche LightCycler®96 (Roche Diagnostics, Switzerland) real-time PCR system according to the manufacturer's protocol. Samples from the same batch experiment of the RNA-seq were used for confirmation experiment. All reactions were performed in triplicate. The qRT-PCR conditions were as follows: 3 min at 95 °C, followed by 45 cycles of 5 s at 95 °C, and 15 s at 60 °C. Dissociation curve analysis was carried out to determine the target specificity. The relative expression of target genes was calculated using the $2^{-\Delta\Delta CT}$ method [16].

Table 2. Primers used for qRT-PCR validation of differentially expressed genes (DEGs).

Gene	Forward Primer (5′-3′)	Reverse Primer (5′-3′)
18S-F	TCTTGATTCGGTGGGTGGTG	CCCGGACATCTAAGGGCATC
CAAP1-F	GTATTCGCTGATCCCCAGCA	GTAACTCACGCCGCAGAAAC
TLR8-F	CTCATCCGCAGGGAGTTGTT	GACCCGCACACAGTTCTACA
TLR13-F	GACCACGGAGGCACACTAAA	CCGGAACCACACAGACAAGA
TLR3-F	CAACCTGACCTCGCTGTCTT	TCTTTCAGCCGGTTCAGTCC
HSP70-F	AGGAGGGTTCAAGAGGGTGT	AATCTCTGCGGTGTGCTTCA
HSP90-F	CCCACCCCGAACTTATTGCT	TGTTCCAGGTTTCCACGCTT
CRT-F	GAAAGCCGCGCTGACTAAAG	AAAGCCTCTCTTGTTGCGGA
Ptp2-F	GTGCAAAGTTGTGCAGGAGG	AAGATGAGGACGAGGACGGA
GSTK1-F	TTGCACACGTCAACGAACAC	ATGGCTGTTCAGGATTGGGG
IRF5-F	TTTCTCCGCATCAAGCCACT	GCCATTGCACCAAGGACAAG
MAP2K6-F	AGCAGGGAAAAGGCAGACAA	AGCTGCCGTGTTATGTGTGA

3. Results

3.1. Transcriptome Sequencing Analysis

Gill tissue transcriptomes were sequenced using Illumina high-throughput sequencing to obtain 219.71G raw bases, and 206.28G clean bases (Table 3) were obtained after filtering, which comprised 93.89% of the original data. The average Q20 and Q30 scores were highest in the spring in ZZ, thereby indicating that the sequence quality was the greatest in this

period. The average Q20 and Q30 scores for the other samples ranged among 95.67–97.55% and 90.11–93.41%, respectively. The GC contents of the samples were 37–46%, which were adequate and thus suitable for subsequent data analysis. The raw data have been submitted in the Sequence Read Archive (SRA) of NCBI with accession number PRJNA1023007.

Table 3. Sequencing data statistics.

Sample	Raw_Bases	Clean_Bases	Q20 (%)	Q30 (%)	GC-Content (%)
ZZ_C_1	7.1G	6.83G	97.23	92.99	39.87
ZZ_C_2	6.88G	6.65G	97.46	93.14	40.33
ZZ_C_3	6.6G	6.4G	97.2	92.63	40.93
ZZ_C_4	6.41G	6.23G	97.55	93.41	37.47
YT_C_1	6.79G	6.49G	96.86	92.54	43.71
YT_C_2	6.96G	6.58G	96.51	91.48	41.71
YT_C_3	7.2G	6.91G	97.08	92.88	41.59
YT_C_4	6.64G	6.45G	97.5	93.08	38.17
ZZ_X_1	7.08G	6.61G	96.67	92.23	44.03
ZZ_X_2	7.16G	6.67G	96.46	91.79	43.81
ZZ_X_3	6.3G	5.78G	96.72	92.51	44.97
ZZ_X_4	6.29G	5.75G	96.83	92.61	45.42
YT_X_1	6.88G	6.32G	96.37	91.7	44.52
YT_X_2	7.01G	6.54G	96.86	92.58	44.46
YT_X_3	6.37G	5.89G	96.64	92.15	44.73
YT_X_4	6.96G	6.29G	96.61	92.11	45.11
ZZ_Q_1	6.95G	6.55G	96.91	92.61	44.64
ZZ_Q_2	6.99G	6.6G	96.98	92.59	45.15
ZZ_Q_3	6.83G	6.42G	97.02	92.68	44.86
ZZ_Q_4	6.92G	6.44G	96.75	92.29	45.8
YT_Q_1	6.83G	6.35G	96.69	92.31	45.61
YT_Q_2	6.95G	6.41G	96.59	92.09	45.95
YT_Q_3	7.02G	6.56G	96.77	92.37	44.19
YT_Q_4	6.73G	6.15G	96.51	91.96	45.43
ZZ_D_1	7.13G	6.74G	96.04	90.74	44.98
ZZ_D_2	6.79G	6.39G	95.64	90.12	44.21
ZZ_D_3	6.97G	6.55G	95.94	90.6	44.69
ZZ_D_4	6.81G	6.36G	95.92	90.52	44.42
YT_D_1	6.47G	6.08G	95.64	90.11	44.56
YT_D_2	7.43G	6.95G	95.99	90.51	44.89
YT_D_3	7.1G	6.67G	96.15	90.97	44.29
YT_D_4	7.16G	6.67G	96.01	90.62	42.31

3.2. Transcription Splicing, Comparison, and Annotation

After removing adapters and low-quality reads using Trinity software, 187,640 unigenes were obtained, with the longest length being 30,252 bp and shortest length being 301 bp. Among them, 80,055 unigenes (42.66%) were less than 500 bp in length, 62,261 (33.18%) were 500–1000 bp, 30,404 (16.20%) were 1000–2000 bp, and 14,920 (7.95%) were greater than 2000 bp (Table 4). The clean data were compared with the unigenes as reference sequences, and the gene expression levels in different seasons were mapped, as shown in Figure 2.

The unigene annotations are shown in Table 5, where 73,085 unigenes were successfully annotated, which accounted for 38.94% of the total unigenes. The numbers of unigenes annotated using the Pfam and GO databases were 51,868 and 51,864, respectively, and they accounted for 27.64% of the total. The number of genes annotated using the Nr database was 38,761, which accounted for 20.65% of the total. After GO enrichment analysis, the unigenes were assigned to three categories comprising biological process, cell component, and molecular function, as well as 42 GO terms, including environmental adaptation, and immune-related terms, such as "response to stimulus" and "immune system process". Most genes were enriched for cellular process and cellular anatomical entity terms (Figure 3).

The enrichment analysis results obtained based on KEGG terms are shown in Figure 4. These unigenes were involved in 34 functional pathways and five categories comprising cellular processes, environmental information processing, genetic information processing, metabolism, and organismal systems. The number of genes enriched for organismal systems was largest (1825), and most genes were involved in regulating the endocrine system and immune system.

Table 4. Summary of transcriptome splicing information.

	Total	300–500 bp	500–1k bp	1k–2k bp	>2k bp	Total Nucleotides	Max Length	Min Length	N50	N90
Transcript	398,505	156,348	130,839	71,522	39,796	383,685,494	30,252	301	1335	420
Unigene	187,640	80,055	62,261	30,404	14,920	165,201,498	30,252	301	1147	399

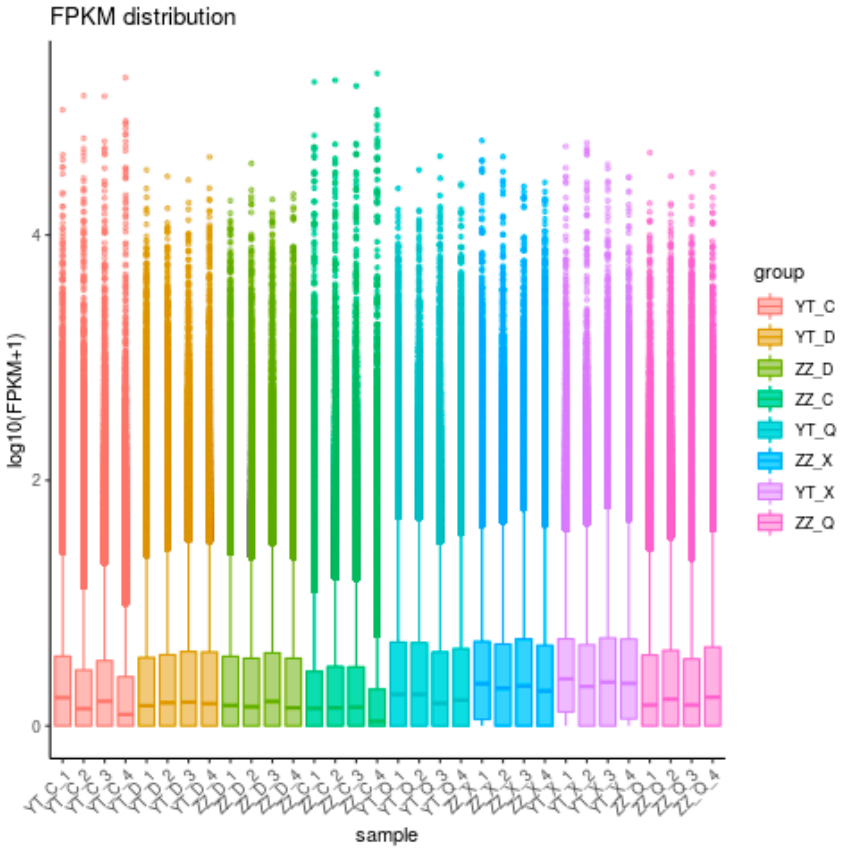

Figure 2. FPKM distribution density of genes in samples under different experimental conditions.

Table 5. Summary of annotations in databases.

	Number of Unigenes	Percentage (%)
NR	38,761	20.65
NT	14,670	7.81
KO	12,238	6.52
SwissProt	19,358	10.31
PFAM	51,868	27.64
GO	51,864	27.64
KOG	9929	5.29
Annotated in all databases	3842	2.04
Annotated in at least one database	73,085	38.94
Total unigenes	187,640	100

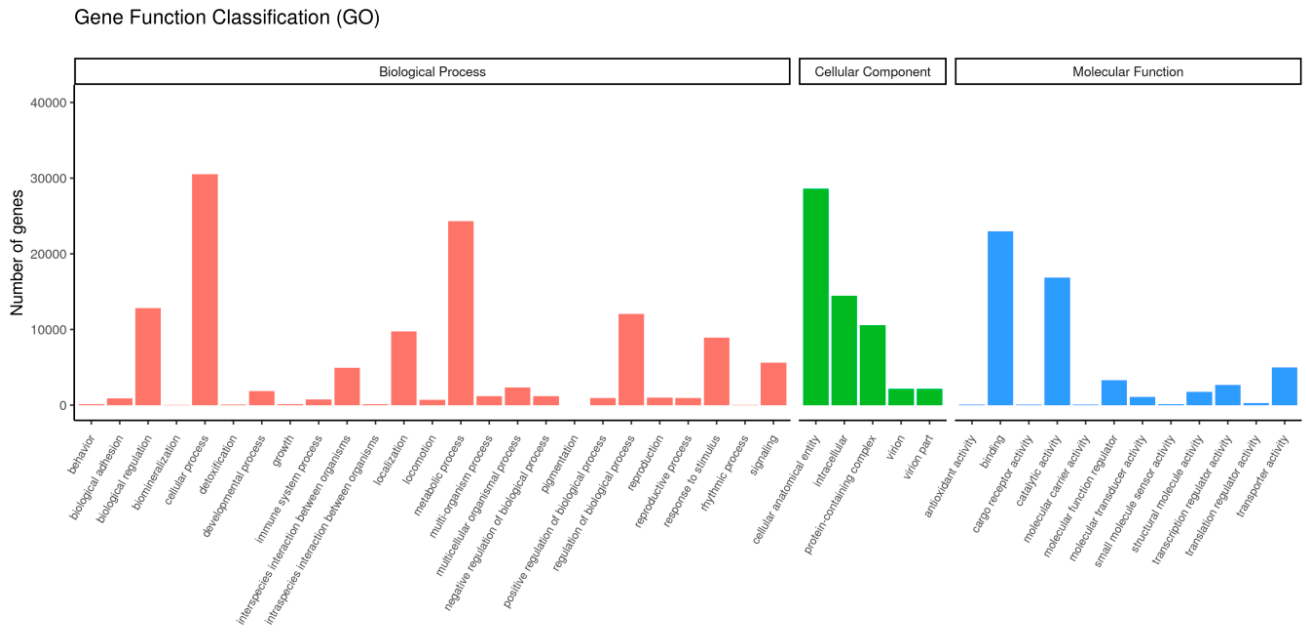

Figure 3. GO annotation categories detected in samples. Biological processes (red), cellular components (blue), and molecular functions (green). The x axis shows the name of the GO entry, with the number of enriched unigenes on the left of the y axis.

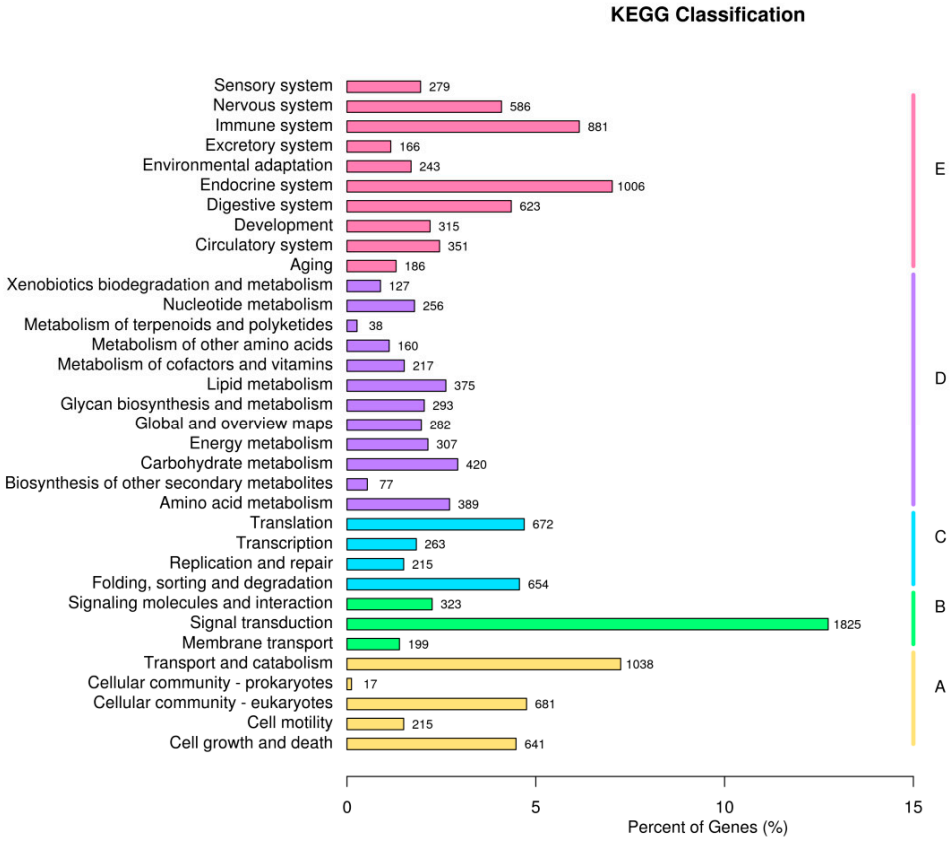

Figure 4. KEGG annotation categories detected in samples. (**A**) Cellular processes; (**B**) environmental information processing; (**C**) genetic information processing; (**D**) metabolism; (**E**) organismal systems.

3.3. Statistics for DEGs

DEGs were screened in gill tissue samples collected from ZZ and YT in the spring, autumn, winter, and summer, and differential gene volcano maps (Figure 5) were drawn. The number of DEGs between ZZ_D vs. ZZ_X was 10,043, with 5461 upregulated genes and 4582 downregulated genes. Among the sampling points in YT, YT_D vs. YT_X had the highest number of DEGs (20,909), with 9503 upregulated genes and 11,406 downregulated genes. The results showed that the number of upregulated genes was higher than that of downregulated genes in most comparisons, and the number of DEGs was highest in the comparison between winter and summer.

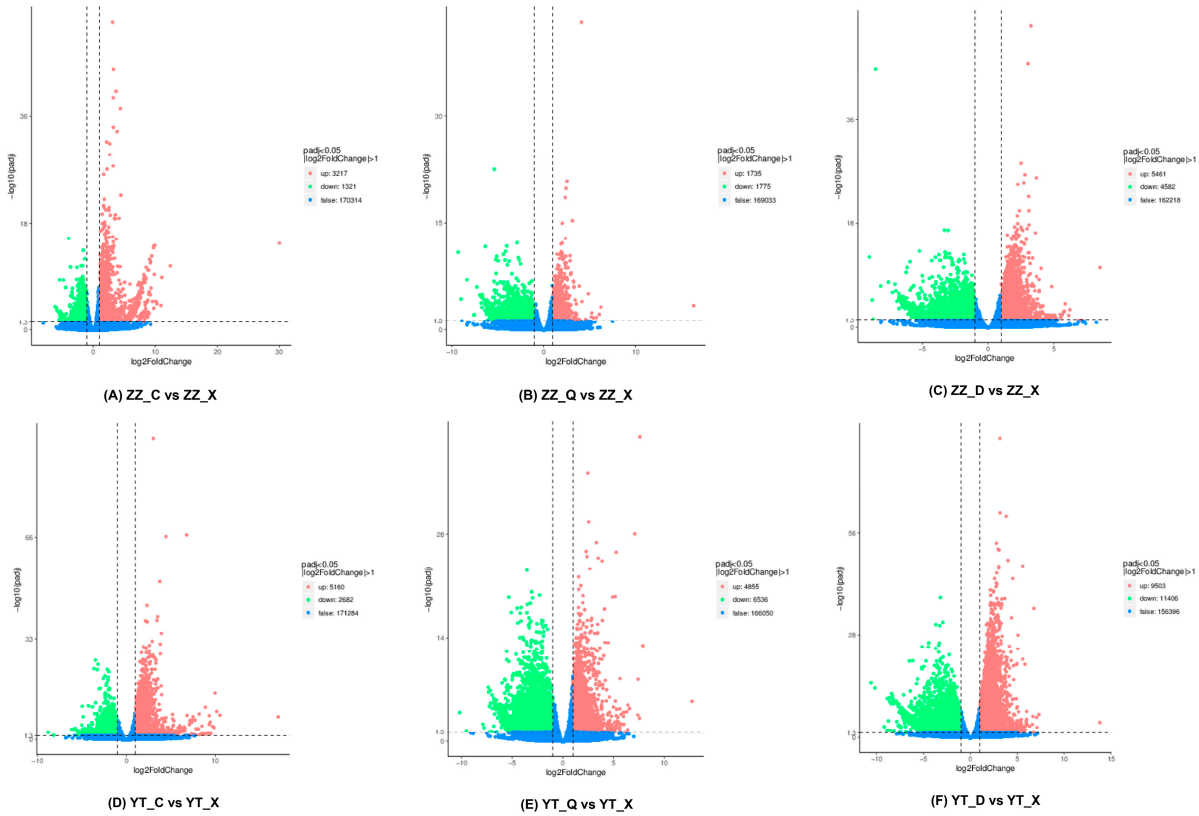

Figure 5. Volcano maps with differentially expressed upper and lower levels between two comparisons. In the figure, the horizontal axis shows the log2foldchange value, and the vertical axis shows −log10padj or −log10pvalue. The dashed blue line represents the threshold differential gene screening criteria, i.e., padj < 0.05 and $|\log2FC| \geq 1$.

3.4. Enrichment Analysis of DEGs

The enriched GO and KEGG terms determined for DEGs screened in ZZ_D vs. ZZ_X and YT_D vs. YT_X are shown in Figures 6 and 7, respectively. GO analysis showed that 16 terms were significantly enriched in ZZ_D vs. ZZ_X, and nine terms were significantly enriched in YT_D vs. YT_X. In particular, many DEGs were related to the cellular nitrogen compound metabolic process and biosynthetic process terms, and only two terms were significantly enriched for cell components in YT_D vs. YT_X. The significantly enriched terms in ZZ_D vs. ZZ_X included an intracellular, protein-containing complex. Among the molecular functions, the significantly enriched terms included oxidoreductase activity and structural constituent of ribosome. The results obtained using KEGG term analysis showed that the enriched pathways included ribosome, spliceosome, and proteasome pathways, and they were related to protein synthesis. Some pathways were related to immunity, such as the cytosolic DNA-sensing pathway and NF-kappa B signaling pathway. It should be noted that the energy metabolism-related pathway for oxidative phosphorylation was

significantly enriched in both comparisons, and terms for many significant disease-related pathways were also enriched.

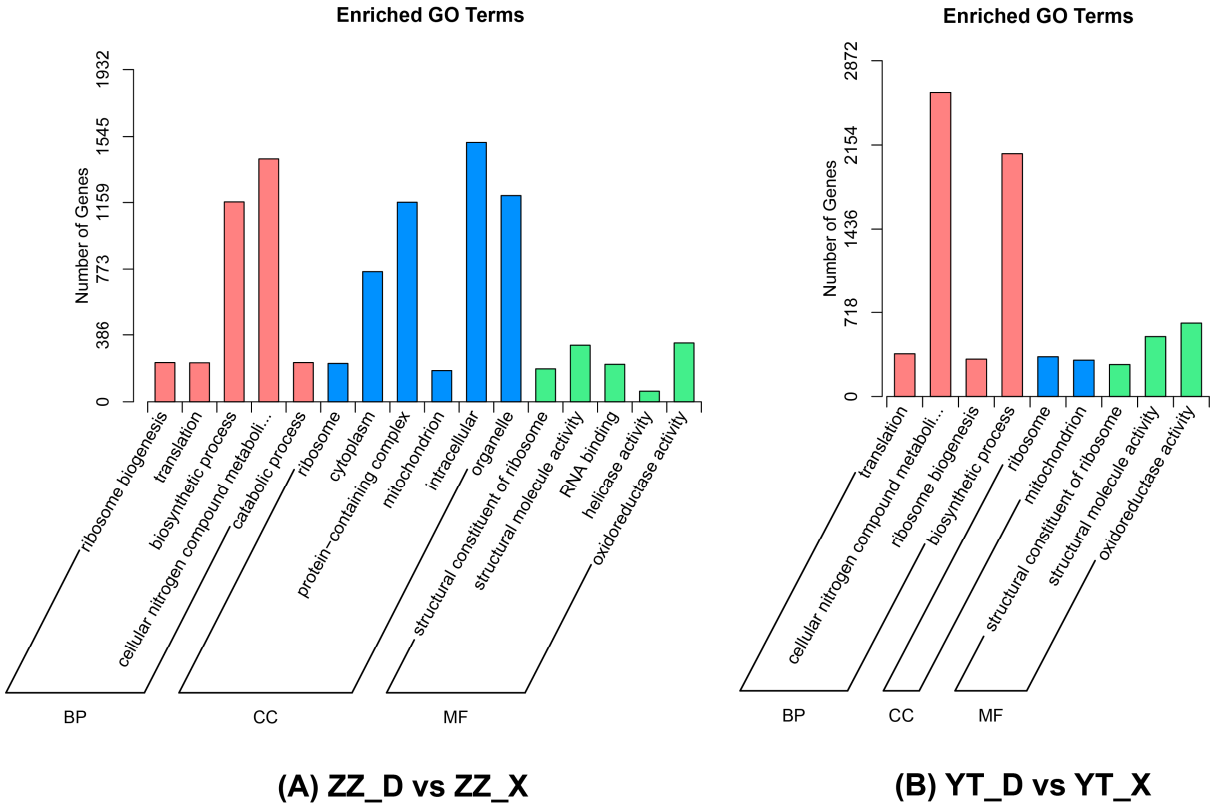

Figure 6. GO categories assigned to DEGs. GO enrichment analysis assigned DEGs to three different categories: biological processes (red), cellular components (blue), and molecular functions (green). The x axis shows the name of the GO entry, with the percentage of downregulated DEGs on the left of the y axis and the number of downregulated DEGs on the right.

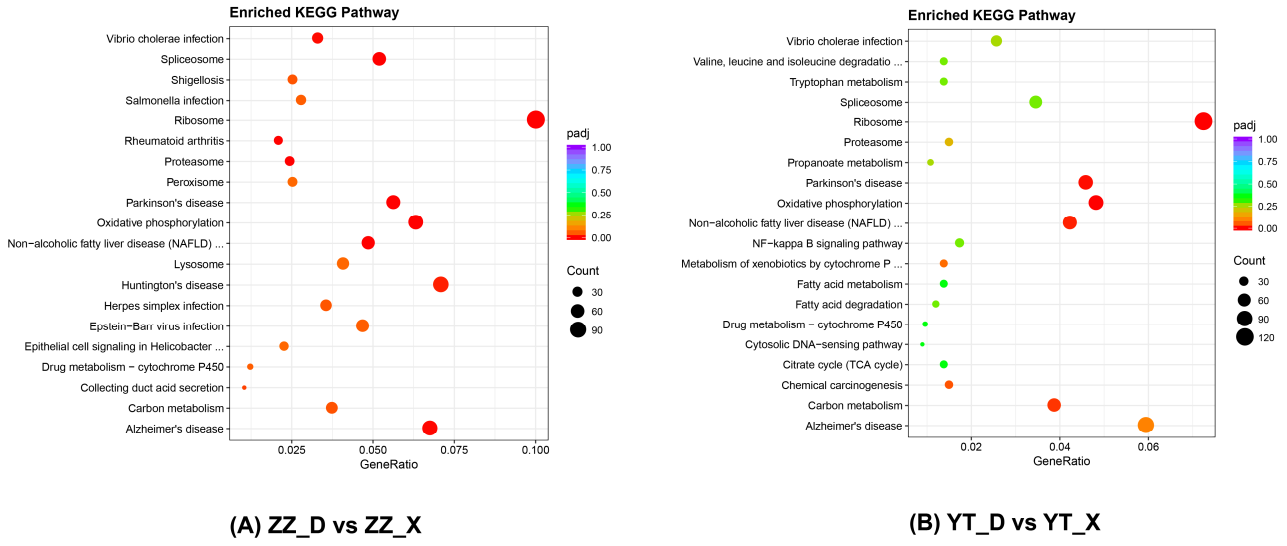

Figure 7. Enriched KEGG pathways. The abscissa represents the enrichment score, and the ordinate is the pathway name. The bubble size indicates the number of DEGs, where larger bubbles indicate pathways with more DEGs. The color represents the size of padj, where a redder bubble color indicates a more significant difference.

3.5. Seasonal Changes in DEGs

We focused on DEGs related to immunity, oxidative stress, and metabolism. We screened 13 immune-related genes, which mainly included pattern recognition receptors, cytokines, phosphatases, and small molecule proteins (Figure 8A). The clustering results showed that the expression levels of most genes were higher in summer and autumn and lower in spring and winter, such as pattern recognition receptors comprising toll-like receptor 2 (TLR2), toll-like receptor 3 (TLR3), interferon regulatory factor IRF5, small molecule protein interleukin 17-like protein (IL-17), and CRT related to apoptosis. We suggest that the high temperature season was more like to promote the expression of these genes, and thus immunity was stronger in summer and autumn. We then screened 12 genes related to oxidative stress, which were mainly assigned to three categories comprising HSPs, mitogen-activated protein kinases (MAPKs), and GSTs (Figure 8B). The results showed that the expression levels of most MAPKs and HSPs increased with the increase in seasonal temperature, such as p38 MAPK, mitogen-activated protein kinase kinase kinase 13-like (MAP3K13), HSP 68-like (HSP68), HSP70, and HSP90. Figure 8 shows that the expression levels of these genes were low in spring, high in summer, and lowest in winter. However, the expression levels of GSTs were relatively low in spring and summer, with gradual increases in autumn, and the highest levels in winter. The nine metabolism-related genes were mainly involved in protein synthesis and energy metabolism (Figure 8C). The expression levels of these genes were highest in winter under low temperature conditions and relatively low in summer under high temperature conditions. We consider that *Neptunea cumingii* can adapt to low temperatures by speeding up its metabolism.

3.6. Validation Snalysis Using qRT-PCR

To validate the sequencing data, 11 DEGs were selected for qPCR analysis (Figure 9). The results showed that IRF5, GSTK1, CRT, TLR8, and CAAP1 were upregulated, whereas HSP90, HSP70, TLR, TLR13, MAP2K6, and Ptp2 were downregulated. The expression patterns of the selected genes detected via qPCR were consistent with the RNA-seq expression profiles, thereby corroborating our results.

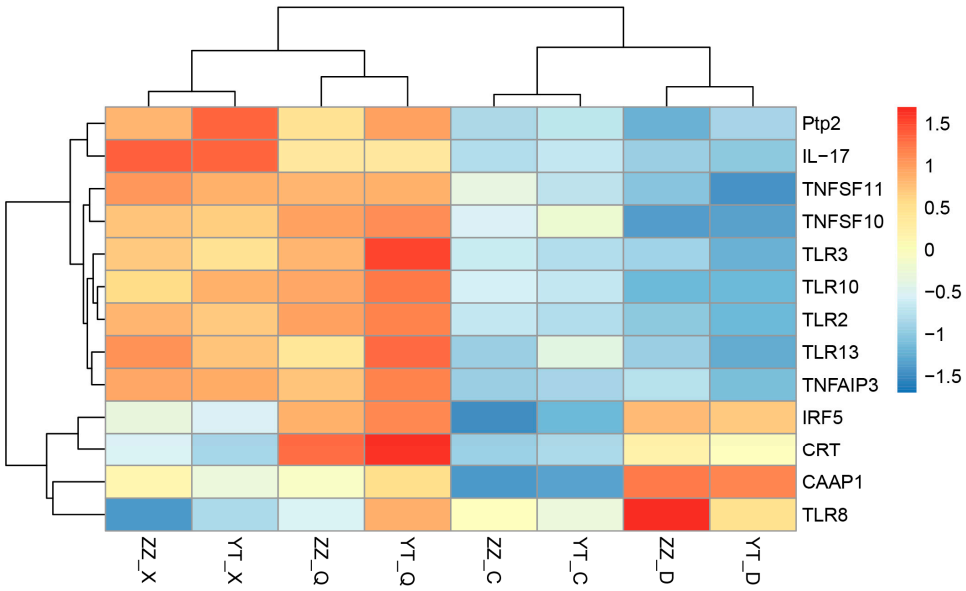

(A) Cluster heat map of immune-related DEGs

Figure 8. *Cont.*

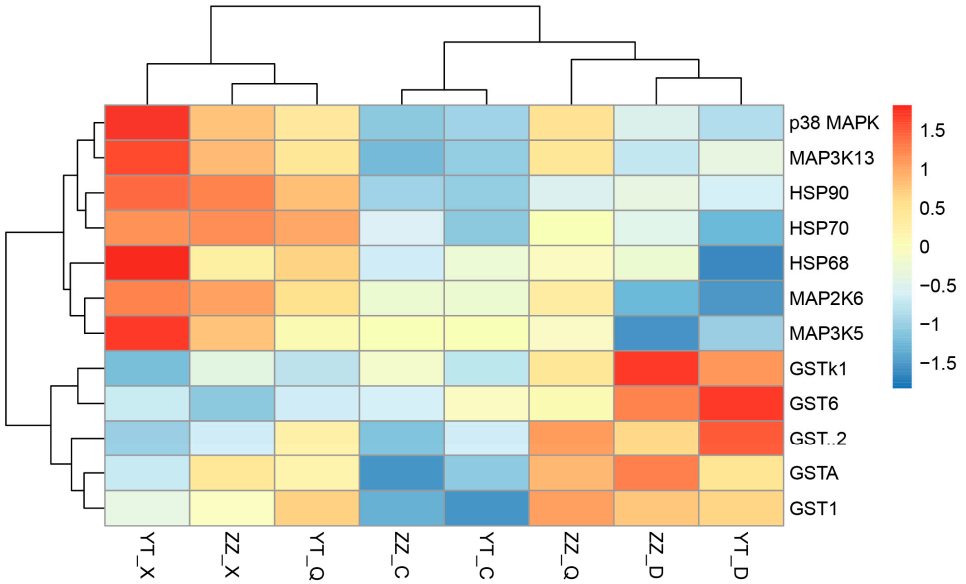

(B) Cluster heat map of oxidative stress related DEGs

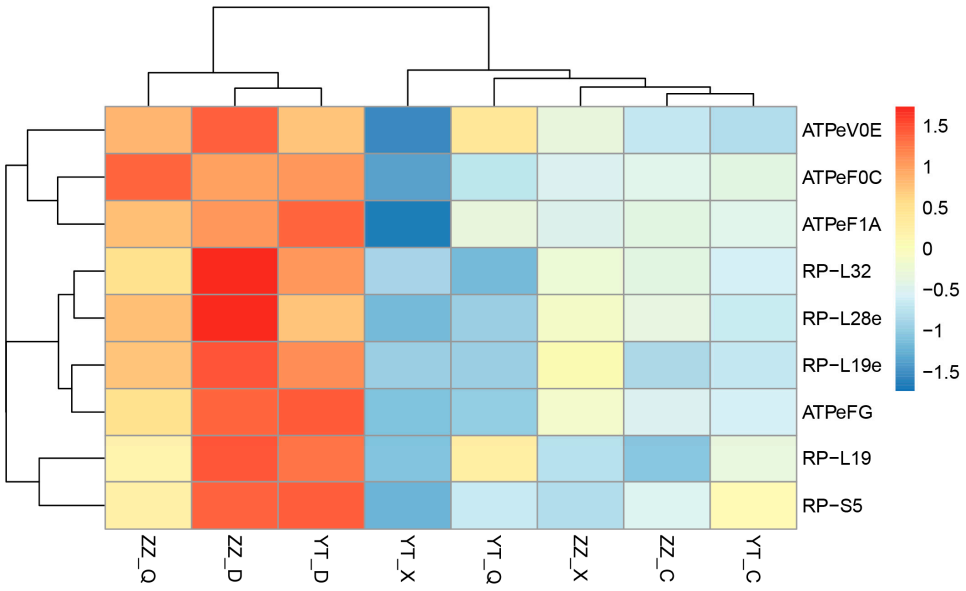

(C) Cluster heat map of metabolism related DEGs

Figure 8. Clustering heat maps of seasonally related DEGs. TNFSF10: tumor necrosis factor ligand superfamily member 10-like; TNFSF11: tumor necrosis factor ligand superfamily member 11-like; TNFAIP3: tumor necrosis factor alpha-induced protein 3; TLR10: toll-like receptor 10. MAP2K6: mitogen-activated protein kinase kinase 6; MAP3K5: mitogen-activated protein kinase kinase kinase kinase 5-like; Gst1: glutathione S-transferase 1-like; Gstθ2: glutathione-S-transferase theta 2-like; GstA: glutathione S-transferase A-like; Gst6: glutathione S-transferase 6. ATPeF0C: f-type H+-transporting ATPase subunit c; ATPeV0E: v-type H+-transporting ATPase subunit e; ATPeFG: f-type H+-transporting ATPase subunit g; RP-L19: ribosomal protein L19; RP-L32: ribosomal protein L32; RP-S5: ribosomal protein S5; RP-L19e: ribosomal protein L19-like; RP-L28e: ribosomal protein L28-like.

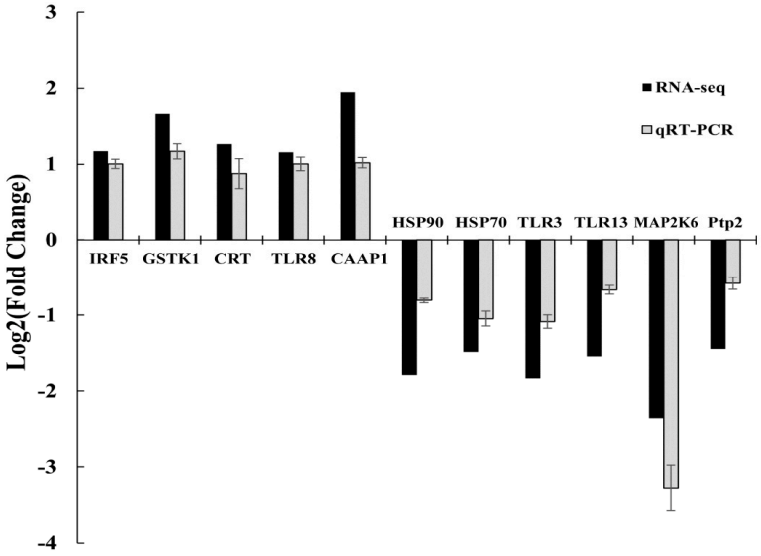

Figure 9. Verification of selected DEGs via qPCR compared with RNA-seq data.

4. Discussion

Temperature is the main environmental factor that affects the immune function and metabolic processes in mollusks [12]. Studies have shown that changes in water temperature can cause significant changes in immune- and metabolism-related genes in shellfish [12,13,17,18]. Gills are the main organs involved in respiration and immune regulation in aquatic organisms [19,20], and they can rapidly sense changes in the water temperature because they are in direct contact with the water environment. Moreover, the large surface area of shellfish gills provides a greater contact area to absorb nutrients in water, thereby facilitating energy metabolism and material exchange. In the present study, transcriptome analysis was conducted using gill tissue samples from *Neptunea cumingii* collected in spring, summer, autumn, and winter to elucidate the regulatory mechanisms related to adaptation to seasonal temperature changes. The results showed that more DEGs were found in the comparison of winter and summer samples, with the highest number of DEGs (20909) for YT_D vs. YT_X. Further screening of DEGs identified thirty-four temperature-related genes, where thirteen played roles in innate immunity, twelve were related to oxidative stress, and nine were related to protein synthesis and energy metabolism. Similarly, Jiang et al. [12] conducted transcriptome analysis based on gill tissues from *Patinopecten yessoensis* under fluctuating water temperatures and found 696 DEGs, including 41 genes related to immunity and 16 genes related to protein metabolism. Furthermore, most of the immune pathways and apoptosis pathways in *Chlamys farreri* were activated under heat stress, where 239 DEGs identified via transcriptome analysis were mostly related to immune signaling pathways [13]. Similar results were obtained in the present study.

In addition, we found that most genes related to immune regulation were highly expressed in summer and autumn when the temperature was higher, with lower expression levels in spring and winter when the temperature was lower, including those of pattern recognition receptor TLRs, transcription factor TNF, and small molecule protein IL-17. Pattern recognition receptors are sensory receptors in organisms that allow them to resist invading pathogens, and they initiate immune responses [21]. TLRs are the main pattern recognition receptors that recognize different pathogen-associated molecular patterns, before triggering signal transduction pathways and regulating the production of antimicrobial peptides [22]. In particular, TLR2 is the main mediator of macrophage activation, where it can recognize various bacterial products and activate the myeloid differentiation factor 88 (MyD88) signaling pathway [23]. In the present study, four types of TLRs (TLR2, TLR3, TLR10, and TLR13) were significantly expressed in summer and autumn, whereas their expression levels were low in spring and winter, thereby indicating that long-term

low temperature conditions reduce the activity of immune factors and increase the susceptibility to pathogens. In addition, our results indicated the inhibition of TNF-family members (TNFSF10, TNFSF11, and TNFAIP3) as downstream signaling intermediates of the TLR's signaling pathway under low temperature conditions in the winter. Similarly, Jiang et al. [12] stimulated *Patinopecten yessoensis* with fluctuating water temperatures and found that TNF was downregulated in the gills and the TLR's pathway was inhibited. TNF can coordinate with the Imd, Toll, and JNK pathways to control the phenoloxidase activity and expression of antimicrobial peptide genes to regulate the innate immune response [24], and the NF-κB signaling pathway is crucial for mediating the cellular TNF response [25]. The NF-κB signaling pathway promotes cell survival by inducing anti-apoptotic gene expression to regulate the body's immune and inflammatory responses [26]. ILs are small molecular proteins secreted by immune cells that play immunomodulatory roles between cells. At present, only two types of ILs [27] comprising IL-12 [28] and IL-17 [29–32] have been found in shellfish. IL-17 plays an important role in regulating the inflammatory response and innate immune response in shellfish. For example, CgIL17–1 can bind to its receptor CgIL17R1 to promote the proliferation of blood lymphocytes in *Crassostrea gigas* [33]. In *Patinopecten yessoensis* [12], IL-17 was significantly downregulated after several temperature fluctuations, and the susceptibility to bacterial infection increased under these conditions. Yang et al. [34] observed the upregulation of IL-17 in *Ctenopharyngodon idella* after high temperature stimulation, thereby indicating that high temperatures could promote the expression of this gene. In the present study, the expression level of IL-17 was higher in summer and lower in winter. We found that the high temperatures in summer promoted the expression of IL-17 in the gills of *Neptunea cumingii*, but the lower temperatures in winter decreased the expression of this gene. In summary, we suggest that metabolism was slow in *Neptunea cumingii* when the water temperature was low in the winter, and thus the immune cell activity was low, and it was more susceptible to infection by pathogens. In shellfish, the immune function is mainly mediated by blood cells. Studies have shown that low temperatures can reduce the cellular immune activity mainly by decreasing cellular metabolism and protein inactivation [35]. In addition, the lower water temperature in winter will decrease the intake of food by shellfish and affect their immune function.

Oxidative stress is a common problem that causes huge economic losses in the animal production industry [36–38]. Oxidative damage is caused by the increased generation of free radicals and/or a decrease in the ability to scavenge them due to disturbance of the oxidation system and antioxidant system, thereby resulting in the accumulation of free radicals in the body [36]. Temperature is one of the main causes of oxidative stress in shellfish. Studies of *Patinopecten yessoensis* [12], *Haliotis discus hannai Ino* [39], *Sinonovacula constricta* [40], *Crassadoma gigantea* [41], *Scapharca broughtonii* [42], and other shellfish have confirmed that temperature can directly affect their antioxidant systems. GST is a key antioxidant enzyme involved in the clearance of reactive oxygen species (ROS), ligand transport, and regulating stress-mediated cell signaling pathways [43]. In the present study, we found that GSTs were significantly expressed at higher levels in the gills of *Neptunea cumingii* under low temperature conditions in the winter, and similar results were also obtained previously for *Pomacea canaliculata*. Lin et al. [44] found that PcGST5 and PcGST11 were significantly upregulated in the hepatopancreas of *Pomacea canaliculata* after cold stress. The production of ROS significantly increased in *Mytilus galloprovincialis* after cold stress at 4 °C ($p < 0.01$), where the peak value was 8.4 times that in the control group [45]. Studies have shown that low temperature can induce oxidative stress in aquatic animals [46], and they may produce more ROS under low temperature stress. Subsequently, the production of GST will be activated in the body to adapt to the increased ROS production. The MAPK signaling pathway plays an important role in mollusk immunity and the response to external environmental stresses [47], and MAPKs are important components of this pathway. In the present study, MAPKs (MAP2K6, MAP3K5, MAP3K13, and p38 MAPK) were expressed at significantly higher levels in the summer but inhibited in the winter, and p38 MAPK is involved in regulating the P38 signaling

pathway. We suggest that, due to the low water temperature in winter, p38 MAPK was inhibited in the gills of *Neptunea cumingii* to affects its cold resistance. Previous studies showed that inhibiting the p38 MAPK activity in zebrafish (*Danio rerio*) could significantly reduce cold resistance by larvae [48], and the apoptosis rate and ROS content of blood lymphocytes were reduced in *Sinonovacula constricta* through P38 MAPK expression [49]. Moreover, Sun et al. found that P38 MAPK could regulate the expression levels of IL-17 and TNF in *Crassostrea gigas* [50,51]. Therefore, we consider that the MAPK signaling pathway is involved in regulating the responses to external environment stresses by shellfish, as well as playing an important role in regulating the immune and inflammatory responses induced by pathogens. In addition, HSPs act as molecular chaperones and play important roles in stress resistance and environmental adaptation [52]. Studies have shown that HSPs are associated with heat resistance by mollusks, and their expression levels are related to the environmental conditions [13]. Thus, HSPs are often used as stress biomarkers [53]. HSPs can also influence the immune response in mollusks by participating in macrophage activation and cytokine or chemokine production [54]. HSP70 and HSP90 are the two main molecular chaperones [53,55,56]. For example, treatment of *Mercenaria mercenaria* via heat stress and hypoxia stress increased the expression levels of HSP90 and HSP70 [57]. Moreover, cold treatment of *Ruditapes philippinarum* [58], *Mytilus galloprovincialis* [45], and *Crassostrea gigas* [59] decreased the expression levels of HSP70 in the gill tissues. In the present study, we found that the expression levels of HSP70 and HSP90 were higher in the gills of *Neptunea cumingii* during the summer. However, these genes were inhibited, and their expression levels were lower under low temperatures in the spring and winter. We suggest that the cold environment negatively affected the transcription of HSPs in the gills of *Neptunea cumingii* by reducing the protein activity levels, disrupting the integrity of organelles, and inhibiting important processes such as transcription and mRNA translation.

Oxidative phosphorylation is an important component of biological energy metabolism. In this process, ADP synthesizes ATP by coupling the energy released via the oxidation of substances in the body with inorganic phosphorus in mitochondria. In particular, 95% of the ATP in the body is produced through oxidative phosphorylation metabolism [60], and it has very important roles in biological growth, metabolism, and environmental adaptability. Oxidative phosphorylation occurs via the electron transfer chain, which is also known as the respiratory chain, in a continuous reaction system comprising a series of hydrogen and electron reactions, where the hydrogen atoms removed by metabolites are transferred to oxygen to generate water, as well as generating ATP [61]. The energy generated through oxidative phosphorylation is strongly related to environmental stress in marine organisms [62]. In the present study, we found that NADH dehydrogenase, V-type H+-transport ATPase subunits (ATPeV0E), and F-type H+-transport ATPase subunits (ATPeF0C, ATPeF1A, and ATPeFG) were significantly upregulated in the gills of *Neptunea cumingii* under low temperatures in the winter. These key enzymes are involved in ATP synthesis and transport, and thus our findings indicate that ATP synthesis and transport were enhanced under low temperatures. Previous studies have demonstrated significant increases in ATPase in the hepatopancreas and gill of *Litopenaeus vannamei* [63] and ATPase in the adductor muscle tissue of *Pinctada fucata martensii* [64] under low temperature conditions. Johnston et al. [65] measured the ATPase activities in the muscles of 19 fish species under long-term, low-temperature stress and found that the ATPase activities were higher compared with those in fish in warm water. In addition, low temperature can lead to reductions in or the loss of enzyme activities, and thus we consider that increasing the transcription of enzymes during oxidative phosphorylation is effective for improving the production of ATPase and slowing decreases in enzyme activities under low temperature conditions. The KEGG enrichment analysis results obtained in this study showed that many DEGs were significantly enriched in the ribosome pathway, and most were ribosomal proteins (RPs). A previous study also showed that the expression of RP-L19 decreased in the gills of *Patinopecten yessoensis* after repeated heat stimulation [12], and similar results were obtained in our study. In particular, the expression levels of several RP genes (RP-S5,

RP-L19, RP-L32, RP-L28e, RPL28, and RP-L19e) decreased under high temperatures in the summer but increased under low temperatures in the winter. Interestingly, the expression patterns of these RP genes differed during the autumn at the two study locations, where the expression levels of these RP genes were upregulated during the autumn in ZZ but downregulated during the autumn in YT, and this difference may have been related to the latitudes of the two locations, and thus further study is required. We suggest that *Neptunea cumingii* adapted to the low temperature environment during the winter by synthesizing RPs, which had stable functions in the subregions of ribosomes [66]. These RPs promoted or inhibited ribosomes in different seasons by replacing damaged subregions in order to ensure the structural and functional stability of ribosomes.

5. Conclusions

In the present study, the transcriptome results were significantly different for the gill tissues of *Neptunea cumingii* in different seasons. The expression levels of immune regulatory genes were promoted in *Neptunea cumingii* during the high-temperature season, whereas the expression levels of genes related to energy metabolism and RP genes were inhibited. Genes related to immune regulation were inhibited in *Neptunea cumingii* during the low-temperature season, and its immunity was relatively low. *Neptunea cumingii* adapted to the low-temperature environment by activating GSTs in the body and accelerating energy metabolism. These results provided a basis for understanding how the molecular defense mechanism of *Neptunea cumingii* might adapt to climate change, as well as a reference for improving the production of *Neptunea cumingii*.

Author Contributions: Z.H. designed the study. D.Z., Y.T. and J.M. performed the study. Y.L. and Y.Z. analyzed the data. Y.Z. wrote the manuscript. All authors have read and agreed to the published version of the manuscript.

Funding: This study was supported by funds from Marine Economy Development Special Project of Liaoning Province Department of Natural Resources, National Natural Science Foundation of China (42076101), Project of Liaoning Provincial Natural Resources Department, the Central Government Subsidy Project for Liaoning Fisheries (2023), and General Project of Education Department of Liaoning Province (LJKZZZ0700).

Institutional Review Board Statement: The animal study was reviewed and approved by University Animal Care and Use Committee of Dalian Ocean University, and the declaration approval number is DLOU2023004.

Data Availability Statement: The datasets presented in this study can be found in online repositories. The names of the repository/repositories and accession number (s) can be found at: https://www.ncbi.nlm.nih.gov/ (PRJNA1023007).

Acknowledgments: The authors wish to express thanks to the staffs of Key Laboratory of Mariculture and Stock Enhancement in North China's Sea, Ministry of Agriculture, China, for their help with the experiment. The authors are also grateful to the reviewers for the great elaboration of the manuscript through their critical reviewing and comments. In addition, the author would like to thank the International Science Editing Company for helping to improve the language ability of this article.

Conflicts of Interest: The authors declare that the research was conducted in the absence of any commercial or financial relationships that could be construed as a potential conflict of interest.

References

1. Qi, Z. Study on the taxonomic flora of benthic invertebrates. *Mar. Sci.* **1979**, *1*, 66–69.
2. Hao, Z.; Wang, Y.; Yu, Y.; Zhan, Y.Y.; Tian, Y.; Wang, L. Analysis and evaluation of nutritive composition in the muscle of *Neptunea arthritica cumingii* Crosse (Gastropoda: Buccinidae). *J. Dalian Univ.* **2016**, *37*, 66–70.
3. Guo, D.; Liu, X.Z.; Wang, A.Y.; Wang, B.; Li, Y.P.; Dong, J. Stock distribution of whelk *Neptunea cumingii* Crosse in Liaodong Bay. *Fish. Sci.* **2015**, *34*, 718–721.
4. Ge, X.; Zhao, J.; Liang, Z.; Chi, Q.; Mao, J.; Wang, X.; Chang, Y.; Hao, Z. Comparative analysis of *Neptunea cumingii* growth, related digestive and immune enzyme indicators, and liver transcriptome under different feeding conditions. *Front. Mar. Sci.* **2022**, *9*, 1013180. [CrossRef]

5. Yu, Y.Y.; Li, J.; Wu, W.; Hao, Z.L. Research progress on the reproductive biology and artificial breeding technology of the *Neptunea cumingii*. *Hebei Fish.* **2019**, *4*, 54–56.
6. Tan, B.; Zhang, D.; Tian, Y.; Mao, J.; Wang, X.; Wang, L.; Chang, Y.; Hao, Z. Genetic structure and local adaptation of *Neptunea cumingii* crosse populations in China based on GBS technology. *Front. Ecol. Evol.* **2023**, *11*, 1154781. [CrossRef]
7. Zhang, Q.H.; Wang, S.J.; Tian, Y.; Wang, L.; Mao, J.X.; Wang, X.B.; Wang, Q.; Chang, Y.; Hao, Z. Effects of dissolved oxygen concentration on behavior, antioxidant enzyme activities and tissue structure of whelk *Neptunea cumingii* Crosse. *J. Dalian Ocean Univ.* **2022**, *37*, 643–649.
8. Zhang, S.Y.; Wang, S.J.; Yang, J.C.; Zhu, J.Y.; Tian, Y.; Wang, L.; Mao, J.; Wang, X.; Chang, Y.; Lu, Z.; et al. Effects of salinity on behavior, activities of antioxidant enzymes and tissue structure of gill and kidney of whelk *Neptunea cumingii* Crosse. *Mar. Sci.* **2022**, *46*, 129–139.
9. Zhang, D.; Dong, X.; Zhu, J.; Yang, J.; Tian, Y.; Wang, L.; Mao, J.; Wang, X.; Chang, Y.; Hao, Z. Effect of water temperature on the behavior of *Neptunea cumingii* and the histology, immune enzyme activity, and transcriptome of its gills and kidneys. *Invertebr. Surviv. J.* **2022**, 1–12. [CrossRef]
10. Jing, H.; Zhou, L.; Gao, Y.; Liu, Z.; Wu, B.; Sun, X.; Tu, K. Transcriptomics and metabolomics reveal the molecular and metabolic adaptation to heat stress in Manila clam *Ruditapes philippinarum*. *Front. Mar. Sci.* **2023**, *10*, 1204598. [CrossRef]
11. Tan, K.; Zhang, B.; Ma, H.; Li, S.; Zheng, H. Oxidative stress responses of golden and brown noble scallops *Chlamys nobilis* to acute cold stress. *Fish Shellfish Immunol.* **2019**, *95*, 349–356. [CrossRef] [PubMed]
12. Jiang, W.; Lin, F.; Fang, J.; Gao, Y.; Du, M.; Fang, J.; Li, W.; Jiang, Z. Transcriptome analysis of the *Yesso scallop*, *Patinopecten yessoensis* gills in response to water temperature fluctuations. *Fish Shellfish Immunol.* **2018**, *80*, 133–140. [CrossRef] [PubMed]
13. Mao, J.; Huang, X.; Sun, H.; Jin, X.; Guan, W.; Xie, J.; Wang, Y.; Wang, X.; Yin, D.; Hao, Z.; et al. Transcriptome analysis provides insight into adaptive mechanisms of scallops under environmental stress. *Front. Mar. Sci.* **2022**, *9*, 971796. [CrossRef]
14. Li, B.; Dewey, C.N. RSEM: Accurate transcript quantification from RNA-Seq data with or without a reference genome. *BMC Bioinform.* **2011**, *12*, 323. [CrossRef] [PubMed]
15. Ren, L.; Zhu, B.Q.; Zhang, Y.B.; Wang, H.Y.; Li, C.Y.; Su, Y.H.; Ba, C.F. The research of applying primer premier 5.0 to design PCR primer. *J. Jinzhou Med. Univ.* **2004**, *25*, 43–46.
16. Livak, K.J.; Schmittgen, T.D. Analysis of relative gene expression data using real-time quantitative PCR and the $2^{-\Delta\Delta CT}$ method. *Methods* **2001**, *254*, 402–408. [CrossRef] [PubMed]
17. Fu, X.; Sun, Y.; Wang, J.; Xing, Q.; Zou, J.; Li, R.; Wang, Z.; Wang, S.; Hu, X.; Zhang, L.; et al. Sequencing-based gene network analysis provides a core set of gene resource for understanding thermal adaptation in Zhikong scallop *Chlamys farreri*. *Mol. Ecol. Resour.* **2014**, *14*, 184–198. [CrossRef]
18. Vosloo, D.; Vosloo, A. Response of cold-acclimated, farmed South African abalone (*Haliotis midae*) to short-term and long-term changes in temperature. *J. Therm. Biol.* **2010**, *35*, 317–323. [CrossRef]
19. Austbø, L.; Aas, I.B.; König, M.; Weli, S.C.; Syed, M.; Falk, K.; Koppang, E.O. Transcriptional response of immune genes in gills and the interbranchial lymphoid tissue of Atlantic salmon challenged with infectious salmon anaemia virus. *Dev. Comp. Immunol.* **2014**, *45*, 107–114. [CrossRef]
20. Havas, M.; Rosseland, B.O. Response of zooplankton, benthos, and fish to acidification: An overview. *Water Air Soil Pollut.* **1995**, *85*, 51–62. [CrossRef]
21. Takeuchi, O.; Akira, S. Pattern recognition receptors and inflammation. *Cell* **2010**, *140*, 805–820. [CrossRef] [PubMed]
22. Arancibia, S.A.; Beltrán, C.J.; Aguirre, I.M.; Silva, P.; Peralta, A.L.; Malinarich, F.; Hermoso, M.A. Toll-like receptors are key participants in innate immune responses. *Biol. Res.* **2007**, *40*, 97–112. [CrossRef] [PubMed]
23. Li, Y.W.; Luo, X.C.; Dan, X.M.; Huang, X.Z.; Qiao, W.; Zhong, Z.P.; Li, A.X. Orange-spotted grouper (*Epinephelus coioides*) TLR2, MyD88 and IL-1β involved in anti-Cryptocaryon irritans response. *Fish Shellfish Immunol.* **2011**, *30*, 1230–1240. [CrossRef] [PubMed]
24. Tang, T.; Li, W.; Wang, X.; Wu, Y.; Liu, F. A house fly TNF ortholog Eiger regulates immune defense via cooperating with Toll and Imd pathways. *Dev. Comp. Immunol.* **2019**, *90*, 21–28. [CrossRef] [PubMed]
25. Tanji, T.; Ip, Y.T. Regulators of the Toll and Imd pathways in the *Drosophila* innate immune response. *Trends Immunol.* **2005**, *26*, 193–198. [CrossRef] [PubMed]
26. Mattson, M.P.; Meffert, M.K. Roles for NF-κB in nerve cell survival, plasticity, and disease. *Cell Death. Differ.* **2006**, *13*, 852–860. [CrossRef] [PubMed]
27. Sun, J.; Song, L. Research progress of inflammation and its pathogenesis in shellfish. *J. Dalian Univ.* **2023**, *38*, 369–379.
28. Xin, L.; Liu, C.; Zhang, H.; Qiu, L.; Wang, L.; Song, L. The characterization of an interleukin-12 p35 homolog involved in the immune modulation of oyster *Crassostrea gigas*. *Dev. Comp. Immunol.* **2021**, *123*, 104145. [CrossRef]
29. Huang, X.D.; Zhang, H.; He, M.X. Comparative and evolutionary analysis of the interleukin 17 gene family in invertebrates. *PLoS ONE* **2015**, *10*, e0132802. [CrossRef]
30. Li, J.; Zhang, Y.; Zhang, Y.; Xiang, Z.; Tong, Y.; Qu, F.; Yu, Z. Genomic characterization and expression analysis of five novel IL-17 genes in the *Pacific oyster*, *Crassostrea gigas*. *Fish Shellfish Immunol.* **2014**, *40*, 455–465. [CrossRef]
31. Saco, A.; Rey-Campos, M.; Rosani, U.; Novoa, B.; Figueras, A. The evolution and diversity of interleukin-17 highlight an expansion in marine invertebrates and its conserved role in mucosal immunity. *Front. Immunol.* **2021**, *12*, 692997. [CrossRef]

32. Wu, S.Z.; Huang, X.D.; Li, Q.; He, M.X. Interleukin-17 in pearl oyster (*Pinctada fucata*): Molecular cloning and functional characterization. *Fish Shellfish Immunol.* **2013**, *34*, 1050–1056. [CrossRef] [PubMed]
33. Cao, W.; Wang, W.; Fan, S.; Li, J.; Li, Q.; Wu, S.; Wang, L.; Song, L. The receptor CgIL-17R1 expressed in granulocytes mediates the CgIL-17 induced haemocytes proliferation in *Crassostrea gigas*. *Dev. Comp. Immunol.* **2022**, *131*, 104376. [CrossRef] [PubMed]
34. Yang, Y.; Yu, H.; Li, H.; Wang, A.; Yu, H.Y. Effect of high temperature on immune response of grass carp (*Ctenopharyngodon idellus*) by transcriptome analysis. *Fish Shellfish Immunol.* **2016**, *58*, 89–95. [CrossRef] [PubMed]
35. Xu, Y.; Wu, W.; Jiang, W.; Ding, Z. Effects of temperature on immune system of shellfish and its mechanisms. *Fish. Sci.* **2012**, *31*, 176–180.
36. Li, H.; Zhong, R.; Fang, Y.; Yang, L. Research progress of oxidative stress and immunity in animals. *Chin. J. Anim. Nutr.* **2014**, *26*, 3217–3221.
37. Mortensen, S.; Strand, Å.; Bodvin, T.; Alfjorden, A.; Skaar, C.K.; Jelmert, A.; Aspan, A.; Saelemyr, L.; Naustvoll, L.-J.; Albretsen, J. Summer mortalities and detection of ostreid herpesvirus microvariant in Pacific oyster *Crassostrea gigas* in Sweden and Norway. *Dis. Aquat. Organ.* **2016**, *117*, 171–176. [CrossRef]
38. Lykkesfeldt, J.; Svendsen, O. Oxidants and antioxidants in disease: Oxidative stress in farm animals. *Vet. J.* **2007**, *173*, 502–511. [CrossRef]
39. Jiang, W.; Fang, J.; Li, J.; Jiang, Z.J.; Mao, Y.Z.; Du, M.R.; Gao, Z.K.; Chen, Q.L. Effects of temperature stress on physiological and biochemical activities of *Haliotis discus hannai Ino*. *J. Fish. Sci. China* **2017**, *24*, 220–230.
40. Hao, S.; Zhang, M. Effects of different cold stress on antioxidant enzyme activity and lipid peroxidation of *Sinonovacula constrictus*. *J. Dalian Univ.* **2020**, *35*, 584–590.
41. Wang, X.; Cao, S.; Liu, G.; Wang, Y.; Zou, J. Effects of temperature on water-free preservation and antioxidant enzyme activity of *Crassadoma gigantea*. *Mar. Sci. Bull.* **2018**, *20*, 1–20.
42. Xue, S.; Wang, J.; Li, J.; Ding, J.; Li, Y.; Xu, H.; Mao, Y.; Fang, J. Effects of temperature on energy metabolism and antioxidant enzyme activities of *Scapharca broughtonii*. *J. Fish. China* **2019**, *43*, 573–583.
43. Kim, M.; Ahn, I.Y.; Cheon, J.; Park, H. Molecular cloning and thermal stress-induced expression of a pi-class glutathione S-transferase (GST) in the Antarctic bivalve *Laternula elliptica*. *Comp. Biochem. Physiol. A Mol. Integr. Physiol.* **2009**, *152*, 207–213. [CrossRef] [PubMed]
44. Lin, Y.; Xiao, Q.; Hao, Q.; Qian, Z.; Li, X.; Li, P.; Li, H.; Chen, L. Genome-wide identification and functional analysis of the glutathione S-transferase (GST) family in *Pomacea canaliculata*. *Int. J. Biol. Macromol.* **2021**, *193*, 2062–2069. [CrossRef] [PubMed]
45. Wang, J.; Ren, R.M.; Yao, C.L. Oxidative stress responses of *Mytilus galloprovincialis* to acute cold and heat during air exposure. *J. Molluscan. Stud.* **2018**, *84*, 285–292. [CrossRef]
46. Malek, R.L.; Sajadi, H.; Abraham, J.; Grundy, M.A.; Gerhard, G.S. The effects of temperature reduction on gene expression and oxidative stress in skeletal muscle from adult zebrafish. *Comp. Biochem. Physiol. C Toxicol. Pharmacol.* **2004**, *138*, 363–373. [CrossRef] [PubMed]
47. Canesi, L.; Betti, M.; Ciacci, C.; Lorusso, L.C.; Pruzzo, C.; Gallo, G. Cell signalling in the immune response of mussel hemocytes. *Invert. Surviv. J.* **2006**, *3*, 40–49.
48. Ren, J.; Long, Y.; Liu, R.; Song, G.; Li, Q.; Cui, Z. Characterization of biological pathways regulating acute cold resistance of zebrafish. *Int. J. Mol. Sci.* **2021**, *22*, 3028. [CrossRef]
49. Wang, Y.; Han, Y.; Wang, Y.; Lv, M.; Li, Y.; Niu, D. Expression of p38MAPK and its regulation of apoptosis under high temperature stress in the razor clam *Sinonovacula constricta*. *Fish Shellfish Immunol.* **2022**, *122*, 288–297. [CrossRef]
50. Sun, J.; Li, Y.; Li, M.; Liu, Y.; Qu, C.; Wang, L.; Song, L. A novel JNK is involved in immune response by regulating IL expression in oyster *Crassostrea gigas*. *Fish Shellfish Immunol.* **2018**, *79*, 93–101. [CrossRef]
51. Sun, J.; Wang, L.; Wu, Z.; Han, S.; Wang, L.; Li, M.; Liu, Z.; Song, L. P38 is involved in immune response by regulating inflammatory cytokine expressions in the Pacific oyster *Crassostrea gigas*. *Dev. Comp. Immunol.* **2019**, *91*, 108–114. [CrossRef] [PubMed]
52. Roberts, R.J.; Agius, C.; Saliba, C.; Bossier, P.; Sung, Y.Y. Heat shock proteins (chaperones) in fish and shellfish and their potential role in relation to fish health: A review. *J. Fish. Dis.* **2010**, *33*, 789–801. [CrossRef] [PubMed]
53. Sørensen, J.G.; Kristensen, T.N.; Loeschcke, V. The evolutionary and ecological role of heat shock proteins. *Ecol. Lett.* **2003**, *6*, 1025–1037. [CrossRef]
54. van Noort, J.M.; Bsibsi, M.; Nacken, P.; Gerritsen, W.H.; Amor, S. The link between small heat shock proteins and the immune system. *Int. J. Biochem. Cell. Biol.* **2012**, *44*, 1670–1679. [CrossRef] [PubMed]
55. Frydman, J. Folding of newly translated proteins in vivo: The role of molecular chaperones. *Annu. Rev. Biochem.* **2001**, *70*, 603–647. [CrossRef] [PubMed]
56. Liu, P.; Lu, Z.; Liu, L.; Li, R.; Liang, Z.; Shen, M.; Xu, H.; Ren, D.; Ji, M.; Yuan, S.; et al. NOD-like receptor signaling in inflammation-associated cancers: From functions to targeted therapies. *Phytomedicine* **2019**, *64*, 152925. [CrossRef] [PubMed]
57. Hu, Z.; Feng, J.; Song, H.; Zhou, C.; Yu, Z.L.; Yang, M.J.; Shi, P.; Guo, Y.-J.; Li, Y.-R.; Zhang, T. Mechanisms of heat and hypoxia defense in hard clam: Insights from transcriptome analysis. *Aquaculture* **2022**, *549*, 737792. [CrossRef]
58. Menike, U.; Lee, Y.; Oh, C.; Wickramaarachchi, W.D.N.; Premachandra, H.K.A.; Park, S.C.; Lee, J.; De Zoysa, M. Oligo-microarray analysis and identification of stress-immune response genes from manila clam (*Ruditapes philippinarum*) exposure to heat and cold stresses. *Mol. Biol. Rep.* **2014**, *41*, 6457–6473. [CrossRef]

59. Zhu, Q.; Zhang, L.; Li, L.; Que, H.; Zhang, G. Expression characterization of stress genes under high and low temperature stresses in the Pacific oyster, *Crassostrea gigas*. *Mar. Biotechnol.* **2016**, *18*, 176–188. [CrossRef]
60. Wang, J.Y.; Zhu, S.G.; Xu, C.F. *Biochemistry*, 3rd ed.; Higher Education Press: Beijing, China, 2002; pp. 114–146.
61. Wang, Z.; Ren, X.; Gao, B.; Liu, P.; Li, J.; Wang, L. Changes in oxidative phosphorylation metabolism of *Portunus trituberculatus* in family inbreeding. *J. Fish. Sci. China* **2018**, *25*, 520–535.
62. Tomanek, L. Proteomics to study adaptations in marine organisms to environmental stress. *J. Proteomics.* **2014**, *105*, 92–106. [CrossRef]
63. Wang, L.; Wang, W.N.; Liu, Y.; Cai, D.X.; Li, J.Z.; Wang, A.L. Two types of ATPases from the Pacific white shrimp, *Litopenaeus vannamei* in response to environmental stress. *Mol. Biol. Rep.* **2012**, *39*, 6427–6438. [CrossRef]
64. Wang, Q.; Liu, Y.; Zheng, Z.; Deng, Y.; Jiao, Y.; Du, X. Adaptive response of pearl oyster *Pinctada fucata martensii* to low water temperature stress. *Fish Shellfish Immunol.* **2018**, *78*, 310–315. [CrossRef]
65. Johnston, I.A.; Frearson, N.; Goldspink, G. The effects of environmental temperature on the properties of myofibrillar adenosine triphosphatase from various species of fish. *Biochem J.* **1973**, *133*, 735–738. [CrossRef]
66. Buckley, B.A.; Gracey, A.Y.; Somero, G.N. The cellular response to heat stress in the goby *Gillichthys mirabilis*: A cDNA microarray and protein-level analysis. *J. Exp. Biol.* **2006**, *209*, 2660–2677. [CrossRef]